Modelling small-patterned neuronal networks coupled to microelectrode arrays

J. Neural Eng. **5** (2008) 350–359 doi:10.1088/1741-2560/5/3/008

Modelling small-patterned neuronal networks coupled to microelectrode arrays

Paolo Massobrio and Sergio Martinoia

Neuroengineering and Bio-Nano Technology Group (NBT), Department of Biophysical and Electronic Engineering (DIBE), University of Genova, Via Opera Pia 11a, 16145 Genova, Italy

E-mail: paolo.massobrio@unige.it and sergio.martinoia@unige.it

Received 22 May 2008
Accepted for publication 1 August 2008
Published 28 August 2008
Online at stacks.iop.org/JNE/5/350

Abstract

Cultured neurons coupled to planar substrates which exhibit 'well-defined' two-dimensional network architectures can provide valuable insights into cell-to-cell communication, network dynamics versus topology, and basic mechanisms of synaptic plasticity and learning. In the literature several approaches were presented to drive neuronal growth, such as surface modification by silane chemistry, photolithographic techniques, microcontact printing, microfluidic channel flow patterning, microdrop patterning, etc. This work presents a computational model fit for reproducing and explaining the dynamics exhibited by small-patterned neuronal networks coupled to microelectrode arrays (MEAs). The model is based on the concept of *meta-neuron*, i.e., a small spatially confined number of actual neurons which perform single macroscopic functions. Each meta-neuron is characterized by a detailed morphology, and the membrane channels are modelled by simple Hodgkin–Huxley and passive kinetics. The two main findings that emerge from the simulations can be summarized as follows: (i) the increasing complexity of meta-neuron morphology reflects the variations of the network dynamics as a function of network development; (ii) the dynamics displayed by the patterned neuronal networks considered can be explained by hypothesizing the presence of several short- and a few long-term distance interactions among small assemblies of neurons (i.e., meta-neurons).

(Some figures in this article are in colour only in the electronic version)

1. Introduction

Cortical networks developing *ex vivo* and coupled to microelectrode arrays (MEAs) represent a valid experimental model to study neuronal dynamics and to understand the principles of brain coding, learning and memory (Marom and Shahaf 2002). Typically, these preparations are characterized by a high neuronal plating density (1200–2000 cells mm^{-2}) and a random connectivity, mediated by excitatory (glutamatergic) and inhibitory (GABAergic) synapses, which evolves continuously during the development (Chiappalone *et al* 2006, Wagenaar *et al* 2006). At the mature stage (i.e., 3rd–4th week in culture), the neurons re-create a highly interconnected network, in which the possibility of inferring functional or actual synaptic connectivity from the recorded activity is prevented by the high cell density. A different approach consists of driving, at least partly, the neuronal network growth (Chang *et al* 2001a, 2001b, Claverol-Tinturé *et al* 2005, 2007, Jun *et al* 2007, Macis *et al* 2007, Liu *et al* 2008), using low-density cultures, and then correlating the dynamic changes of the network activity with its topology and synaptic connectivity.

From a modelling point of view, several approaches can be taken into account to describe neuronal network dynamics. A possible method consists of using interconnected point neurons (Giugliano *et al* 1999, Gerstner 2003, Izhikevich 2003), neglecting all the morphological and anatomical details of the neuronal structures. In this way, since the

computational bottleneck is the spatial integration along the compartmentalized neurons, it is easy to implement large-scale neuronal networks made up of thousands of units (Kowalsi *et al* 1992, Latham *et al* 2000, Segev and Ben-Jacob 2001, Izhikevich *et al* 2004, Persi *et al* 2004, Volman *et al* 2004, Vogels and Abbot 2005, Vogels *et al* 2005, Raichman *et al* 2006, Parga and Abbot 2007). In this framework, the fundamental role is played by general topology rules. Several types of architecture were proposed in the literature to model the neuronal network connectivity, such as scale-free, random, small-world, syn-fire chains or more complex structures which drive the network dynamics to different states (Mehring *et al* 2003, Abeles *et al* 2004, Shin and Kim 2006, Parga and Abbot 2007, Teramae and Fukai 2007). However, these models are particularly valuable to simulate large-scale neuronal networks where no evident or clear information on the connectivity is available, then it is necessary to formulate hypotheses about the network architecture.

In this work, we propose an alternative approach to describe the dynamics exhibited by patterned neuronal networks. To this goal, we considered a simplified neuronal network model made up of a few representative units (*meta-neurons*) in which the morphological aspects (e.g., dendritic arborization and length) were taken into account. A *meta-neuron* represents a small number of actual neurons (i.e., an assembly of spatially confined neurons) which perform a single macroscopic function. From a modelling point of view, a meta-neuron can be described by a detailed compartmental model with its proper connections. By this approach, it is not necessary to simulate all the actual neurons of the network (i.e., thousands of neurons), but it is relevant to represent the functional connections found in these preparations. Thus, following this strategy, we implemented simplified networks, made up of 60 meta-neurons synaptically connected, in order to emulate the dynamics experimentally obtained by ad hoc patterned neuronal networks (Macis *et al* 2007). Each element was coupled to a microelectrode position, and the network was mapped to reflect the number of recording sites in a MEA device.

All the simulations were carried out in the NEURON environment (Hines and Carnevale 1997, Carnevale and Hines 2005), and the model listing can be downloaded from our web page (http.//www.bio.dibe.unige.it).

The spontaneous activity as well as the evoked responses obtained by focal electrical stimulation was simulated and characterized by means of the typical statistics used for describing the experimental data, i.e., mean firing rate (MFR), mean bursting rate (MBR), interburst interval (IBI) distribution and post-stimulus time histogram (PSTH) (Rieke *et al* 1997). The obtained results were then compared with the experimental ones found in the actual patterned neuronal networks.

In this way, we showed that the overall dynamics of such constrained networks can be captured by a reduced number of neurons with proper connectivity and specific morphology.

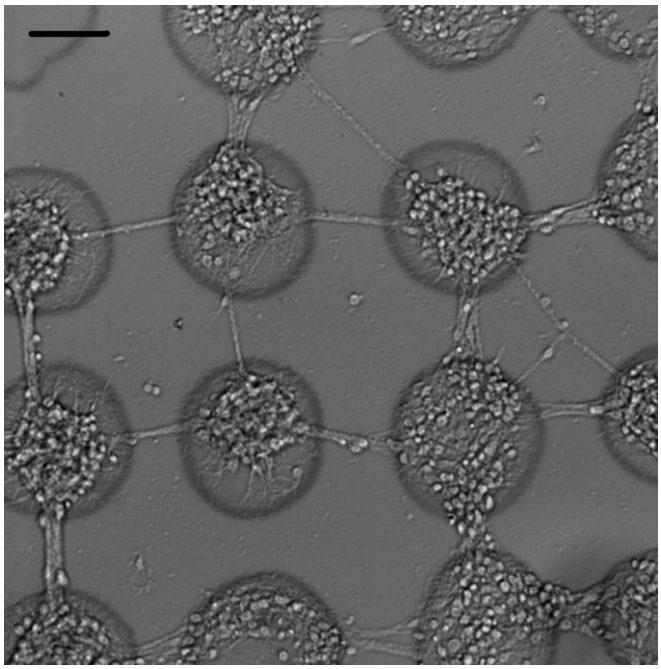

Figure 1. Superimposition of the fluorescence image of the FITC-labelled poly-l-lysine spots deposited on a glass coverslip surface with the differential interference contrast (DIC) image of interconnected neuronal systems grown on them. The presence of bundles of neurites which interconnect the sub-populations of neurons is clearly evident. The scale bar is 100 μm.

2. Cell cultures and experimental set-up

Dissociated neuronal cultures were obtained from cerebral cortices of embryonic rats, at gestational day 18 (E18). After an enzymatic and mechanical trituration, cells were plated onto 60-channel MEAs (Multi Channel Systems, Reutlingen, Germany), precoated with patterned adhesion promoting molecules (poly-l-lysine and laminin). The generated droplets had a diameter size of about 60–80 μm corresponding to a volume in the range of 100–300 pl. The stabilized neurons, developed in correspondence with the deposited micro-islands of adhesion molecules, defined neuronal aggregates of 60 cells per island, on average. More details about the microdrop deposition technique can be found in Macis *et al* (2007). Figure 1 shows that neurons are anchored on the substrate only in the areas where the adhesion proteins were deposited. Among these areas, the cells formed interconnected sub-populations which clearly appear during the later stages of development (i.e., 3rd–4th week in culture). This process typically occurs by almost bridging gaps among nearest neighbouring clusters. The interconnections among adjacent neuronal sub-populations are constituted by bundles of neurites (axons and dendrites).

3. The models

3.1. Model of the neuron

The morphologies of the neuron models designed in NEURON (Carnevale and Hines 2005) are shown in

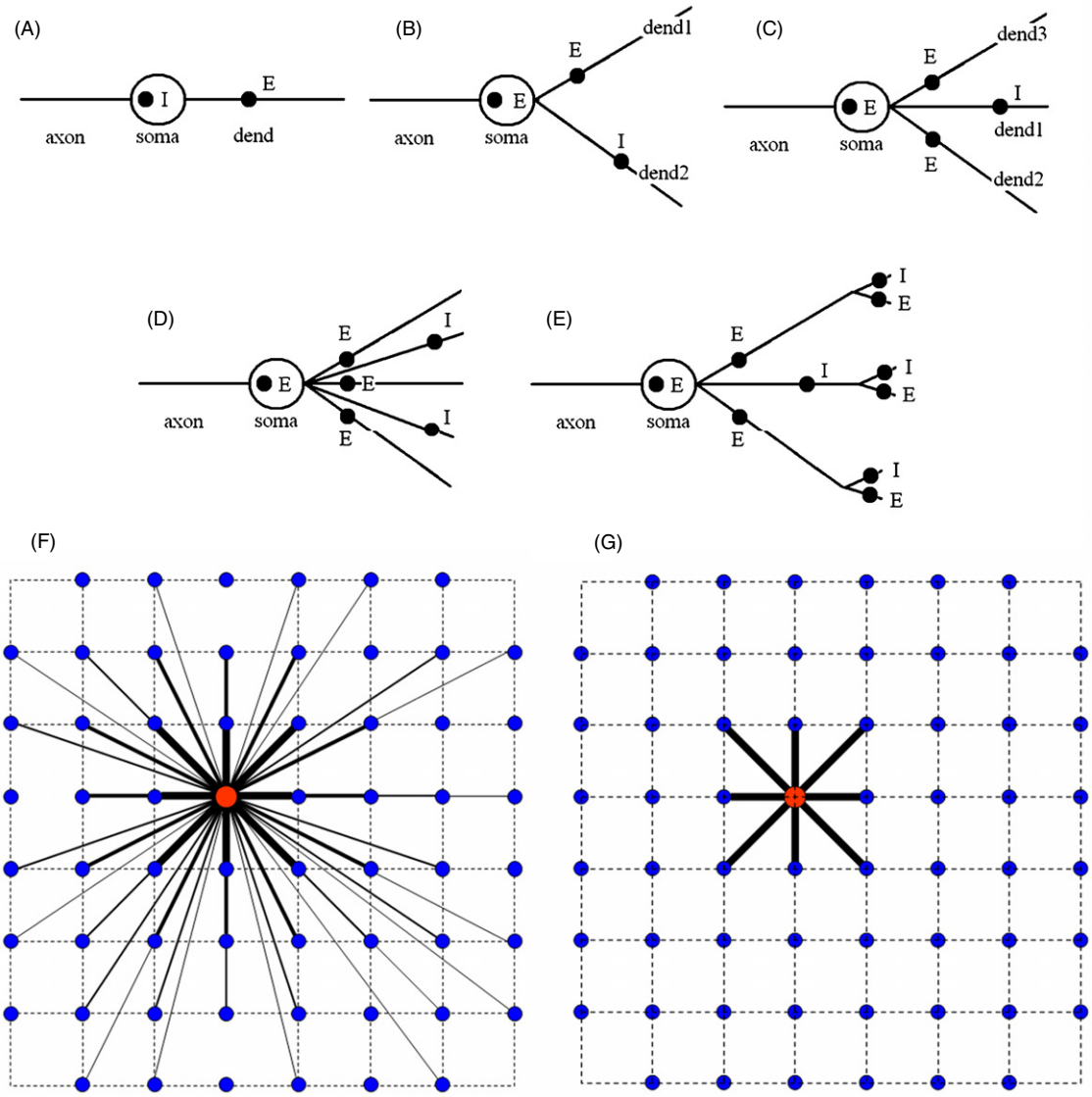

Figure 2. Sketches of the different neuron models and different network architectures. Each neuron is made up of a soma, an axon and a variable number of dendrites. In particular, (A) 1 dendrite, (B) 2 dendrites, (C) 3 dendrites, (D) 5 dendrites and (E) 9 dendrites distributed over two levels. (F) A sketch of the network model organized by following the OTM rule: the red dot identifies a representative meta-neuron connected to many others (blue dots). The different thickness of the edges represents the number of connections (i.e., the thicker the edges, the higher the number of connections). In this way, adjacent meta-neurons are the most connected and then the synaptic efficacy is increased. (G) A sketch of the network model organized by following the OTN rule: only adjacent meta-neurons are connected.

figure 2; all the neuronal structures were made up of a soma, an axon and a dendritic tree with different degrees of complexity. The geometrical dimensions (length and diameter) of each neuronal section were set as follows: soma (30 μm, 30 μm), axon (1000 μm, 1 μm), proximal dendrites (1000 μm, 2 μm) and distal dendrites (500 μm, 2 μm) (London *et al* 1999, Van Ooyen *et al* 2002).

The electrophysiological properties of the neuronal membrane are based on the Hodgkin–Huxley (H–H) model (Hodgkin and Huxley 1952) for the soma and axon, and on a passive electrical model for the dendrites. Under these assumptions, the neuronal membrane total current density i_{mem} obeys the following equation:

$$i_{\mathrm{mem}} = C_{\mathrm{mem}} \frac{\mathrm{d}V_{\mathrm{mem}}}{\mathrm{d}t} + \sum_i i_i. \tag{1}$$

In (1), C_{mem} is the membrane capacitance, V_{mem} is the membrane potential and i_i is the current density originated by the flow of the ith ionic species through the ith membrane channel. In general, the current flowing through each channel is described by the relation

$$i_i = \alpha \cdot \bar{g}_i \cdot (V_{\mathrm{mem}} - E_i). \tag{2}$$

In (2), $\bar{g}_i$ is the maximum channel conductance of the ith ion, E_i is its equilibrium potential and α is a dimensionless parameter that can assume different mathematical expressions according to the type of channel (Hodgkin and Huxley 1952). In particular, α is a function of time t and membrane potential V_{mem} if the H–H model holds; it assumes the unity value if the passive model holds.

Moreover, the compartmental model approach (Segev *et al* 1989) was taken into account in the model definition; all

the compartments are isopotential and show an equal length of 10% of the space constant ($\lambda = 50\ \mu$m) of the neuron membrane.

The following neuronal membrane parameter values were assumed in the simulations: membrane capacitance $C_{\mathrm{mem}} = 1\ \mu\mathrm{F\ cm^{-2}}$, axoplasmatic resistance $R_a = 160\ \Omega$ cm, sodium and potassium maximum ionic conductances $\bar{g}_{\mathrm{Na}} = 120\ \mathrm{mS\ cm^{-2}}$ and $\bar{g}_{\mathrm{K}} = 36\ \mathrm{mS\ cm^{-2}}$, respectively, leakage conductance $g_l = 0.3\ \mathrm{mS\ cm^{-2}}$, sodium, potassium and leakage ionic equilibrium potentials $E_{\mathrm{Na}} = 50$ mV, $E_K = -77.5$ mV and $E_l = -54.3$ mV, respectively.

3.2. Model of the synapse

The model of the synapse follows the approach proposed in Destexhe *et al* (1994). Such an approach is based on the first-order kinetic scheme:

$$R + T \xleftrightarrow{K_1, k_2} TR^* \tag{3}$$

which describes the binding of the neurotransmitter molecules T released by the presynaptic neuron when an action potential occurs to postsynaptic receptors R. In (3), R and TR^* are the unbound and bound forms of the postsynaptic receptor, respectively, and k_1 and k_2 are the forward and backward rate constants for transmitter–receptor binding. The fraction of the bound receptors r is described by the equation

$$\frac{\mathrm{d}r}{\mathrm{d}t} = k_1 \cdot [T] \cdot (1 - r) - k_2 \cdot r. \tag{4}$$

This modelling approach allowed the synaptic events to be represented by equations with the same structure of the H–H equations. The parameters of the kinetic synapse model were derived from physiological measurements. In the simulations, the duration of the excitatory and inhibitory neurotransmitter release in the synaptic cleft was set to 1.1 and 1.08 ms, respectively (Colquhoun *et al* 1992), and the kinetic constant values k_1 and k_2 for excitatory and inhibitory synapses were set to 10, 1 $\mathrm{ms^{-1}\ mM^{-1}}$ and 0.5, 0.02 $\mathrm{ms^{-1}}$, respectively. The synapses (inhibitory and excitatory) were placed on the soma and on the dendrites of the neuron models, as depicted in figure 2.

3.3. Model of the neuronal network

The models of the neuron and synapse described in the previous sections were used to simulate the dynamics exhibited by small-patterned neuronal networks.

The network model is made up of 60 meta-neurons arranged according to the MEA layout (an 8×8 square grid, without the four corner electrodes). Each neuron can establish synaptic connections, as shown in figure 1, also preserving the ratio between excitation and inhibition (60–75%). Synapses are placed on the soma and on the dendrites: in this way, axo-dendritic and axo-somatic connections were taken into account as typically happens in actual cortical cultures (Marom and Shahaf 2002).

In order to investigate the possible mechanisms which drive the connectivity among the clusters of neurons by means of bundles of neurites (cf figure 1), we considered two different connectivity rules, namely *one-to-many* (OTM) and *one-to-neighbours* (OTN).

The OTM rule states that each meta-neuron can establish several random connections (both excitatory and inhibitory) to the neighbours (maximum value: 30) and few connections (minimum value: 0) as far as the distance increases; the closer the two meta-neurons are, the more connected they are, and thus the synaptic efficacy of the connection is increased.

The OTN rule defines a local connectivity and states that each meta-neuron is only connected to its nearest neighbours (up to eight meta-neurons). A simplified representation of the OTM and OTN connectivity rules is depicted in figures 2(F) and (G), respectively.

4. Data analysis

The first step in the data analysis procedure consisted of the spike detection in the simulation outputs. This operation was performed by means of a simple hard-threshold algorithm: a threshold of 0 mV was set to identify a spike. Then, the same statistical parameters used for describing the experimental data were applied to the generated spike trains (Rieke *et al* 1997).

All the post-processing analyses were achieved by using custom-developed software implemented in Matlab (The Mathworks, Natick, MA, USA). In particular, the statistics applied to the simulated and recorded signals in order to characterize and study the bursting and spiking behaviour of the neuronal networks were mean firing rate (MFR), mean bursting rate (MBR) and interburst interval (IBI) distribution. Finally, the evoked activity was analysed by means of the post-stimulus time histogram (PSTH) (Rieke *et al* 1997).

5. Results

The following sections present the simulation results of the neuron morphologies described in section 3.1, both in their isolated and connected configurations to define a neuronal network.

5.1. Simulation of the neurons in their isolated form

Each neuron of figure 1 exhibits its own peculiar spiking activity if considered in its isolated form, as predicted by the Hodgkin and Huxley model. Under this operating condition, the simulated spiking activity of the soma of the neurons in a configuration with 1, 3, 5 and 9 dendrites is shown in figure 3. Simulations were carried out by applying a current stimulus of 1.2 nA amplitude and 100 ms duration.

The isolated neurons show a spiking activity for the neuronal morphology characterized by 1 and 3 dendrites (cf figures 3(A) and (B), respectively). If the complexity of the dendritic tree is enhanced, the firing frequency decreases (cf figure 3(C)) until only one spike appears at the onset of the current stimulus (cf figure 3(D)), showing a phasic spiking behaviour. However, the absence of bursts or clusters of spikes followed by silent periods is quite evident, which is typical in cultured dissociated neurons (Wagenaar *et al* 2006).

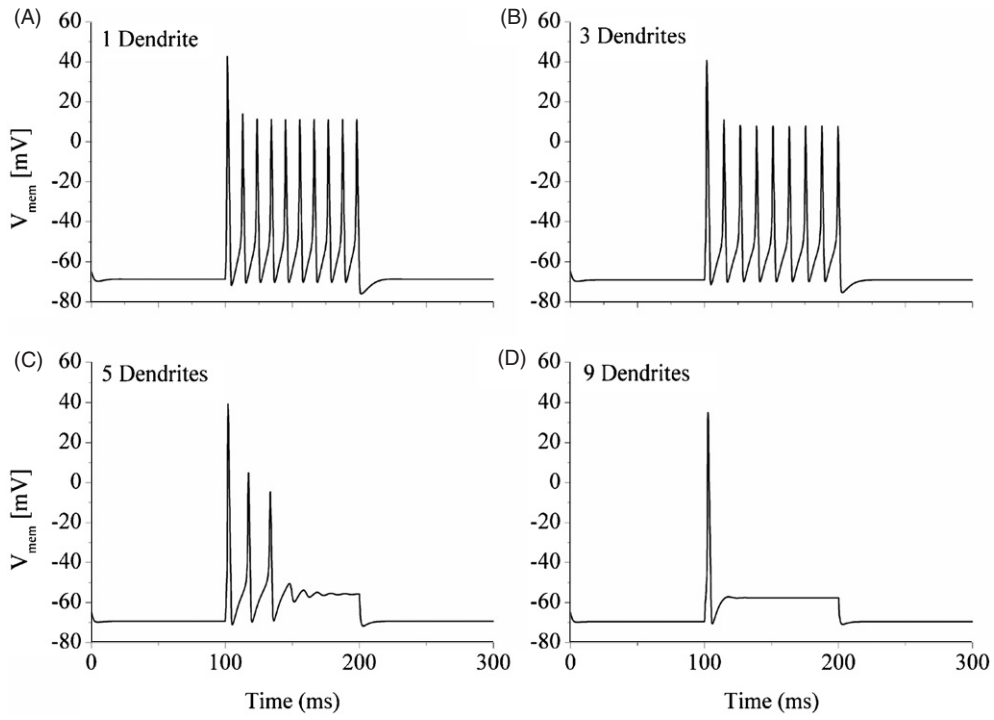

Figure 3. Simulated spiking activity obtained by considering neurons in their isolated form. A spiking activity with adaptation behaviour is observed by increasing the complexity of the dendritic tree. Electrophysiological activity is elicited by means of a current stimulus pulse (amplitude 1.2 nA, duration 100 ms). (A) 1 dendrite, (B) 3 dendrites, (C) 5 dendrites and (D) 9 dendrites.

5.2. Simulation of spontaneous activity

The electrophysiological behaviour of the neurons changes dramatically when they are connected to make a network. *In vitro*, neuronal networks are spontaneously active, i.e., they exhibit electrophysiological activity even without electrical or chemical stimulation. To simulate the condition of spontaneous activity, we added a Gaussian noise source to the leakage channels of each component of the neuron models of figure 2. Neurons are intrinsically noisy and several sources were identified (for a review, see Faisal *et al* (2008) and references therein). The most dominant source of such electrical noise is channel noise, i.e., electrical currents caused by the random opening and closing of the ion channels (Steinmetz *et al* 2000, White *et al* 2000).

From the results of the simulation of spontaneous activity, we obtained two important findings regarding the dynamics exhibited by patterned neuronal networks. The results pointed out that it is possible to switch from a spiking to a bursting behaviour by enhancing the morphology of the meta-neurons. Thus, since these electrophysiological patterns are strictly dependent on the network development (Chiappalone *et al* 2006, Wagenaar *et al* 2006), we are able to reproduce different stage of maturation. Finally, we looked for possible architecture rules which could guarantee such dynamics in patterned neuronal networks.

5.2.1. The complexity of the meta-neuron morphology is correlated to the development of the network. In order to analyse the effects of the meta-neuron morphology on the global electrical activity of the neuronal network, the dendritic complexity of the neuron models (cf section 3.1) is varied according to the OTM connectivity rule (cf section 3.3).

The simulated action potentials of one (randomly chosen) of the 60 neurons of the four networks obtained by varying the morphology of the dendritic tree are shown in figure 4. Each plot takes into account the same time interval of 2 s over a total simulation time of 60 s (sampled at 10 kHz). Figure 4(A) (1 dendrite per neuron) shows a recorded low electrical activity that suggests the network activity seems to be ruled by isolated spikes. An increase of the number of dendrites makes the network behaviour change dramatically: in the configuration with 3 dendrites per neuron, the network exhibits a tonic activity (cf figure 4(B)) with a high firing rate. At a further increase of the number of dendrites (5 or 9), clusters of spikes (bursts) spaced out by silent periods were obtained (cf figures 4(C) and (D)). Analogous plots (not shown) were obtained from the other 59 neurons of the network. We also increased further the dendritic complexity (neurons with 12, 15 and 20 dendrites) and we obtained similar results to those obtained for neurons with 9 dendrites, thus suggesting a sort of saturation phenomenon (data not shown).

From these simulations, synchronized bursting events called *network bursts* appear (Van Pelt *et al* 2004, 2005, Chiappalone *et al* 2006, Raichman and Ben-Jacob 2008). As it happens in the experimental conditions, dissociated cortical neurons in the mature stage fire in a synchronous way, and the spreading activity tends to involve all the microelectrodes of the MEA. This suggests that the dendritic complexity, the number of connections and the ratio between excitatory and inhibitory synapses induce a global bursting behaviour although neuron models are intrinsically spiking.

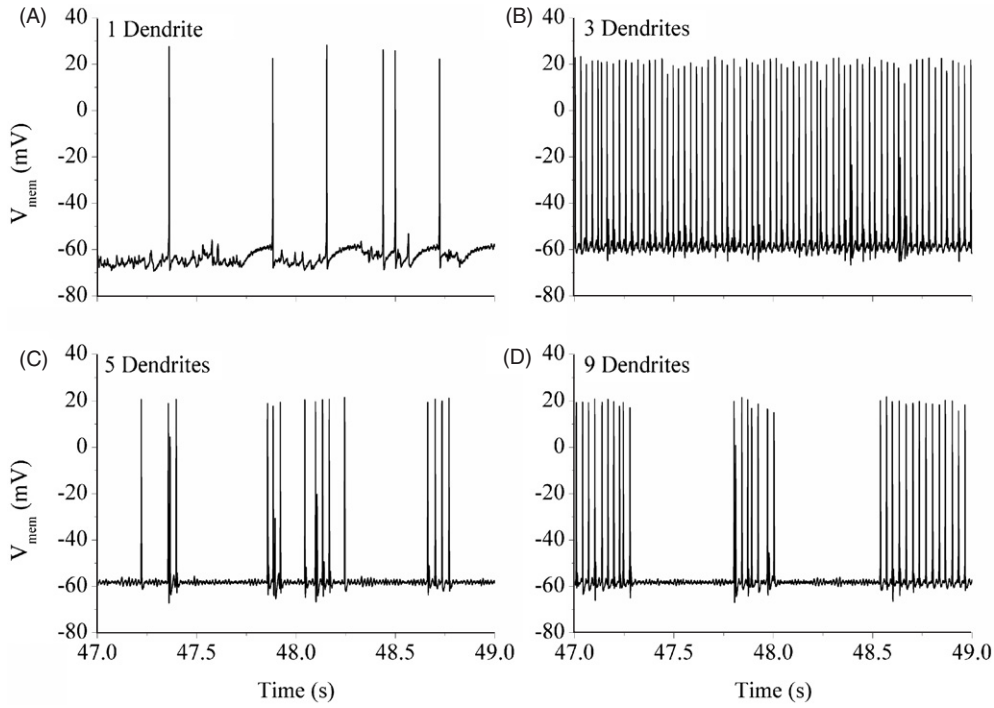

Figure 4. Simulated spiking activity of one randomly chosen neuron of the four neuronal networks obtained by varying the dendritic arborisation. It is evident that when increasing the number of dendrites the electrophysiological activity switches from isolated spikes (A) to tonic spiking (B) up to clusterized spikes (C, D).

To validate the proposed model, the simulation results were compared with the experimental data obtained from patterned cortical networks on different days *in vitro* (DIVs) of development.

Figure 5(A) shows the MBR and the MFR of the simulated network (OTM connectivity rule) as a function of the complexity of the dendritic tree. In particular, it can be noticed that the MFR reaches high values (40–45 spikes s^{-1}) in the case of neurons with 2 or 3 dendrites (tonic activity), but it decreases to 12 spikes s^{-1} in the case of neurons with 1 dendrite. An understanding of the MFR trend shown in figure 5(A) can be helped by also considering the MBR trend (figure 5(A), square symbol); this analysis justifies the apparent incongruity of the results in the case of 5 dendrites which can be ascribed to the presence of silent periods (no spikes) that lower the MFR. A saturation behaviour of the network is also evident from figure 5: if the number of dendrites is increased above the critical value of 9, it seems that the network behaviour reaches a stable state. Figure 5(A) shows results for up to 12 dendrites.

The simulated results of the MFR and MBR of the networks made up of neurons with 1 and 5 dendrites were close to those experimentally observed: considering a data set of five patterned neuronal networks, we found an MFR $= 7.21 \pm 1.05$ spikes s^{-1} and an MBR $= 17.47 \pm 2.13$ bursts min^{-1} (mean $\pm$ standard deviation).

To completely characterize the influence of the meta-neuron morphology on the neuronal activity, simulations were performed by varying the geometrical characteristics. The results (data not shown) indicate that by increasing the dendrite length an increase of the electrical activity was observed, both in terms of spiking and bursting activity (a change in the burst's shape in terms of duration and amplitude was observed); moreover, by varying the dendrite diameter, no appreciable variations were detected.

To make a comparison with the actual patterned neuronal networks, we characterized the simulated neuronal dynamics by means of the IBI distribution. Figures 5(C) and (D) compare the simulated results obtained from networks ruled by the OTM connectivity and made up of neurons with 1 and 5 dendrites, respectively, with the neuronal dynamics obtained by recording the electrophysiological activity of patterned neuronal networks at different degree of maturation (i.e., 14 and 27 DIV). The results underline the change of the dynamics which occurs accordingly to the different degree of cellular and network development (by means of synaptic interactions). In fact, at an early stage of development (14 DIV), a mixed activity characterized by random spikes and bursts arises as shown by the IBI distribution of figure 5(C). Such electrophysiological patterns are well modelled by simple neuron morphology with a minimal dendritic tree (only one dendrite). On the other hand, a maturation of the neuron structure (neurons made up of 5 dendrites) makes the network more bursting, as shown by the simulated IBI distribution of figure 5(D); the simulated results well fit the experimental data obtained from a mature patterned culture of 27 DIVs old.

To underline how the neuron morphology is relevant to the proposed meta-neuron modelling approach, a simple network made up of 60 point neurons described by the well-known Izhikevich model (Izhikevich 2003) was designed. In particular, the parameters of the Izhikevich model were set equations to reproduce regular spiking and fast spiking for

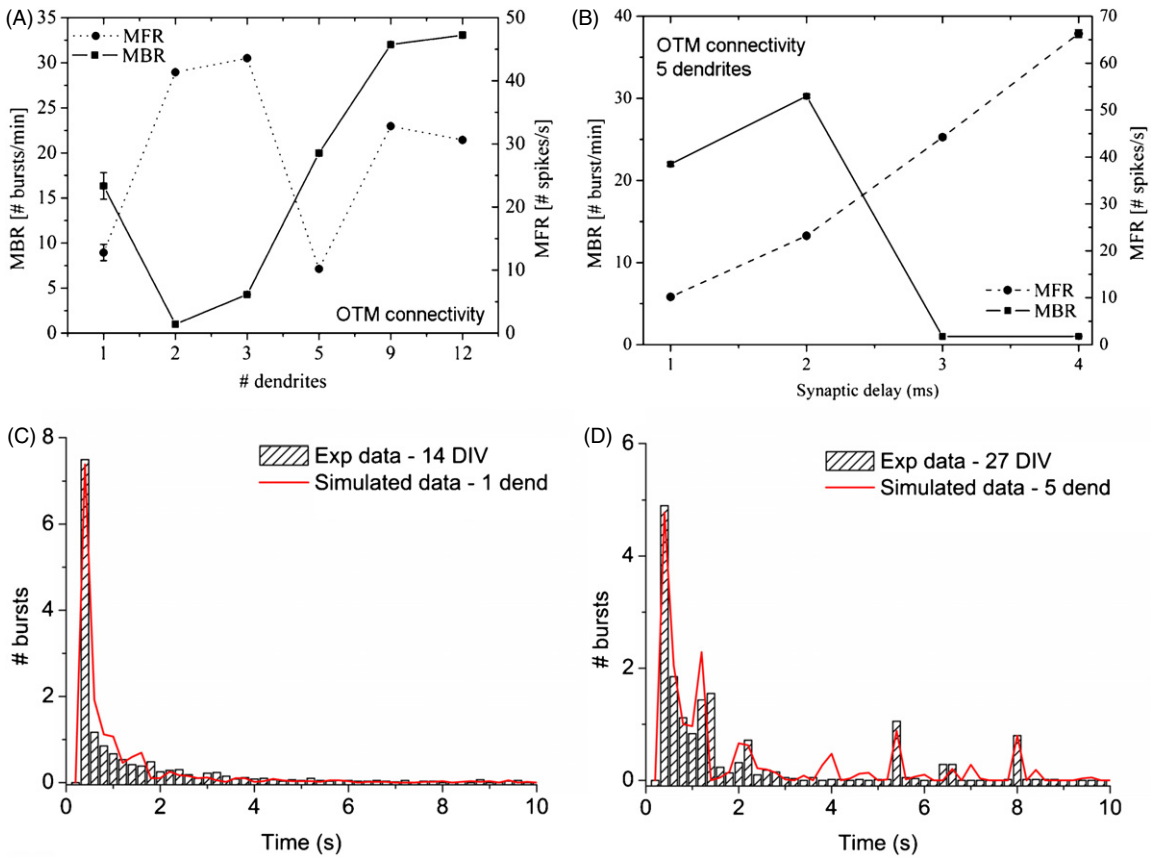

Figure 5. (A) MFR (dot) and MBR (square) of the simulated neuronal network as a function of the number of dendrites when the network connectivity follows the OTM rule. (B) MFR (dot) and MBR (square) as a function of the synaptic delay. (C, D) IBI distribution of simulated data (red lines), considering different neuronal morphologies, and experimental dynamics, sampled at different DIVs (bars). Simulation results are pertinent to a network following the OTM rule.

excitatory and inhibitory neurons, respectively (Izhikevich *et al* 2004). The network connectivity was driven by the OTM and OTN rules as described in section 3.3. Simulations were performed by sweeping the synaptic weights, the synaptic delay and the subthreshold background stimulation used to induce spontaneous activity. We found that by varying the synaptic weights and delay in a wide range (1–50, 1–4 ms, respectively), a very low firing frequency was achieved (MFR < 0.9 spikes s^{-1}), with the consequence that the bursting activity was totally absent; moreover, several neurons were completely silent for the entire duration of the simulation (number of active neurons <5). This low-frequency activity can be changed by increasing the background stimulation. However, a threshold behaviour emerged: at low-current values, the network keeps on remaining silent or firing at low frequency. On the other hand, if a threshold is exceeded, a high-frequency tonic firing appears (MFR > 30 spikes s^{-1}) and all the neurons are active. The obtained simulation results (not shown) confirm that a large number of point neurons are necessary to capture the electrophysiological activity patterns shown by these specific patterned neuronal preparations.

5.2.2. Switching from spiking to bursting activity is also associated with synaptic delays. The aforementioned simulation results dealt with the dendritic complexity of the neuron model. To better understand which other factors could induce the neuronal dynamics to switch from spiking to bursting activity (or to a mixed mode), we varied the synaptic delay from 1 to 4 ms, which are typical physiological values experimentally taken (Marom and Shahaf 2002). To achieve this goal, we implemented a neuronal network made up of 60 meta-neurons, each with 5 dendrites, ruled by the OTM connectivity. The simulated result is shown in figure 5(B) where the MFR and MBR are plotted as a function of the synaptic delay. The MFR and the MBR display the opposite trend: an increase of the synaptic delay induces a monotonic increment of the MFR, whereas the MBR, after reaching its maximum for 2 ms, decreases dramatically, as indicated in Shao *et al* (2006). This behaviour can be explained by supposing the existence of a synaptic delay threshold (between 2 and 2.5 ms). If this value is exceeded, the network switches to a behaviour dominated by a tonic activity, where no bursts are present. This observation is strengthened by the analysis of the coefficient of variation (CV) of the interspike interval distribution (ISI): for a synaptic delay of 2 ms CV assumes a value of 0.84, whereas for 3 ms the CV value decreases to 0.09. This means that the electrophysiological activity switches from an irregular state (where random spikes and bursts are present) to a state dominated by regular spiking.

5.2.3. Impact of the connectivity rules on the network dynamics. All the previous simulations were performed

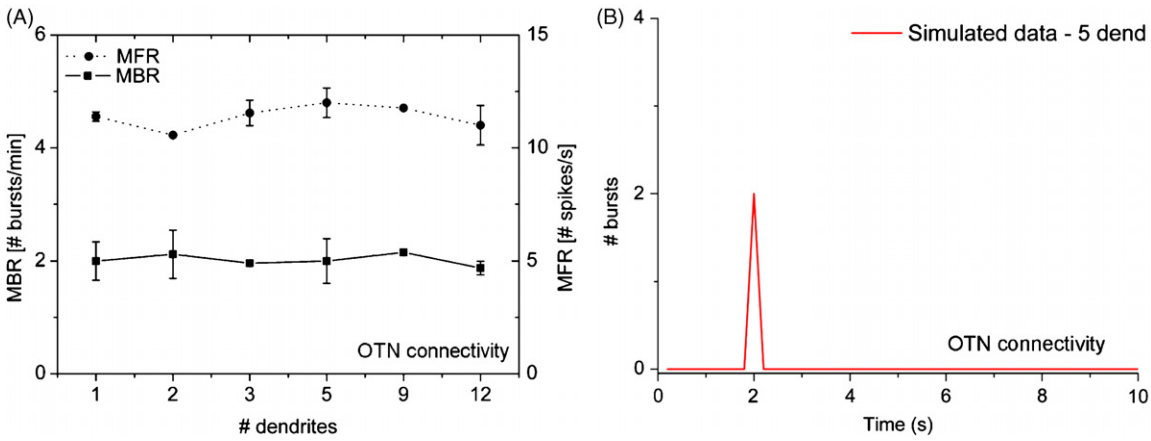

Figure 6. (A) MFR (dot) and MBR (square) of the simulated neuronal network as a function of the number of dendrites when the network connectivity follows the OTN rule. The role of the dendritic morphology on the network dynamics vanishes. (B) Also the IBI distribution, in the case of OTN ruled networks, presents an unrealistic trend, suggesting that the OTM rule is preferred in patterned neuronal networks.

considering a connectivity described by the OTM rule (cf section 3.3). We asked ourselves if the neuron assemblies depicted in figure 1 could be connected by an OTN rule (cf section 3.3), where each assembly is only connected to its nearest neighbours. Thus, we simulated networks made up of 60 meta-neurons ruled by the OTN connectivity, with the same number of dendrites used in the OTM configuration.

The same statistics and analyses previously used for the network model in the OTM connectivity configuration were applied to these simulated results. The main result is that this kind of network architecture makes the role of the dendritic arborisation less relevant: in fact, sweeping the number of dendrites from 1 to 12, an MFR $=$ 11.37 ± 0.21 spikes s^{-1} and an MBR $=$ 2.01 ± 0.04 bursts min^{-1} (mean $\pm$ standard deviation) (figure 6(A)) were obtained. The IBI distribution, relative to the case of a network made up of meta-neurons each with 5 dendrites, shows a different trend from those experimentally found: only one peak is present in correspondence of $t = 2$ s, suggesting quite different and not very realistic dynamics (figure 6(B)).

5.3. Simulation of the evoked activity

Generally, to test if the network is capable of responding to the electrical stimulation, a low-frequency (0.2–0.5 Hz) test stimulus is delivered from some active electrodes (Marom and Shahaf 2002, Wagenaar *et al* 2005, Massobrio *et al* 2007).

Referring to the cluster of microelectrodes in figure 7(A), voltage stimuli, i.e., biphasic rectangular voltage pulses (width 250 μs; peak-to-peak amplitude 1.5 V; frequency 0.2 Hz), were applied to electrode 67. The response of the network was analysed by the PSTHs as shown in figure 7(B). As it might be expected, electrodes 55 and 56 showed site-specific responses reflecting the functional topographical connectivity of the network: electrode 55, the closest one to the stimulating site, showed a fast response, whereas electrode 56, slightly further apart, exhibited a more delayed response. Moreover, electrodes 37, 46 and 58 produced an attenuate response to the stimulus or, in some cases, no evoked activity (electrodes 38, 45, 47, 48).

The network model (made up of 60 meta-neurons each with 5 dendrites) ruled by the OTM connectivity, designed and tested for the spontaneous activity simulation, was used to emulate the experimental condition of focused electrical stimulation. We reproduced the electrical stimulation protocol by means of a current stimuli pulse (width 100 ms; peak-to-peak amplitude 1.0 nA; frequency 0.2 Hz) delivered to one meta-neuron (upper-right corner). As obtained from the experimental conditions, the efficacy of the stimulation involved primarily the adjacent electrodes (figure 7(C)). In fact, the electrodes closest to the stimulation site present a fast and marked response, whereas the others can present a more delayed and attenuate response, or in some case, no evoked activity.

Finally, to demonstrate that OTM connectivity is more realistic than OTN connectivity, this stimulation protocol was applied to a network model organized following this kind of topology. The results shown in figure 7(D) highlight that the propagation of the evoked response is confined only to the first next neighbours meta-neurons. A mild response involving all the far meta-neurons is practically absent or negligible.

6. Discussion and conclusions

In this work, we proposed a neuronal network model made up of neurons (i.e., *meta-neurons*) with appropriate morphology (number of dendrites, length of neurites) and connectivity, able to capture the dynamics of specifically patterned neuronal networks. The main feature of the model is the introduction of such meta-neurons with their own defined morphology which are coupled to specific microelectrodes and which can be combined with specified connectivity rules.

In particular, we showed that a specific morphology (i.e., a certain number of compartments) and connectivity (i.e., OTM) are necessary to implement a suitable network model.

We tested the proposed model by comparing the simulation results with the experimental data obtained from

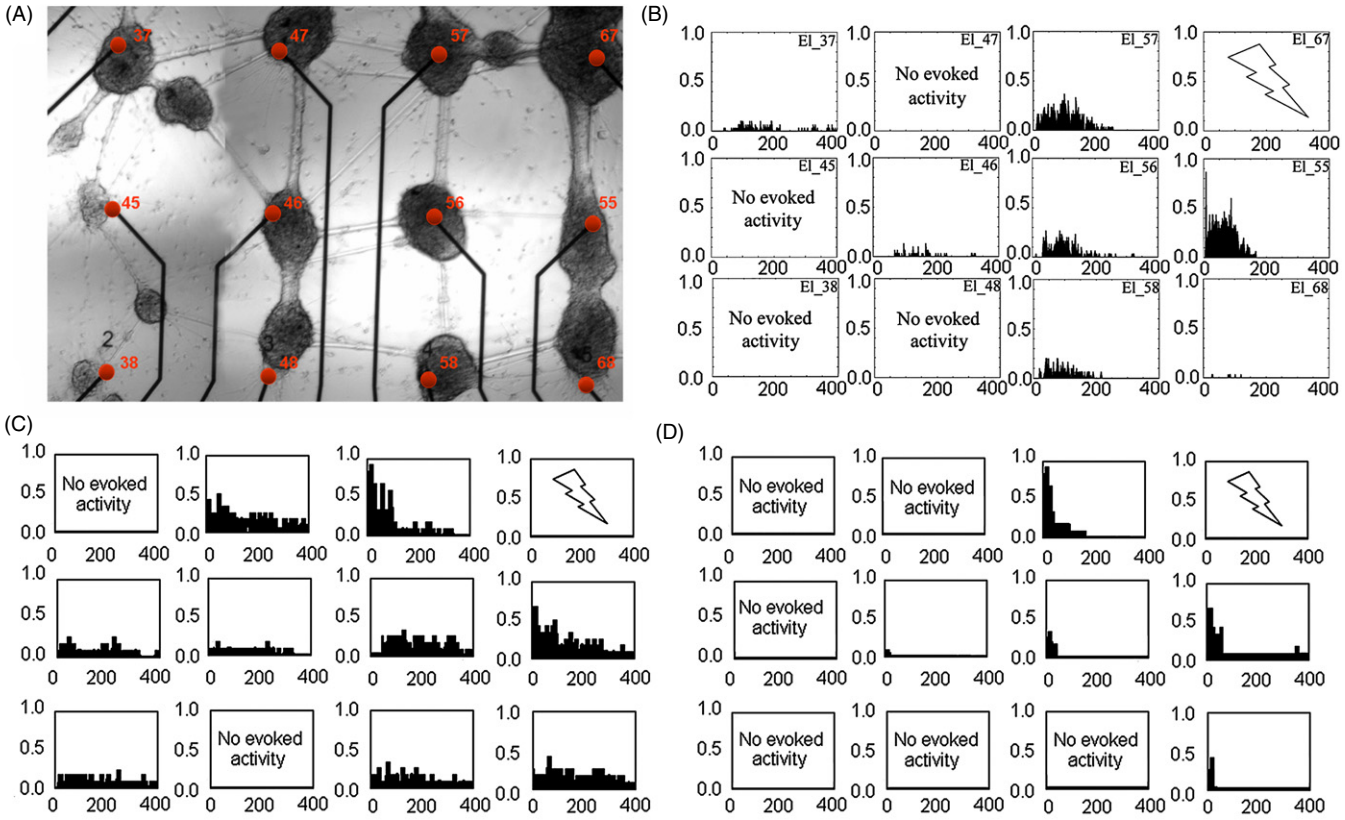

Figure 7. (A) DIC image of a neuronal network at 27 DIV on an MEA. The scale bar is 100 μm. (B) PSTHs relative to the culture depicted in (A). Electrical stimulation, delivered from electrode 67 (upper-right corner), especially involves the adjacent electrodes, decreasing to 0 as the distance increases. (C) The simulated neuronal network (organized following the OTM rule) described in section 3.3 shows a similar behaviour to that experimentally obtained. (D) In contrast, if the simulated neuronal network follows the OTN rule, the evoked response is exclusively confined to the adjacent meta-neurons.

patterned networks realized with a recently introduced microdropping technique (Macis *et al* 2007). We demonstrated that the model can be tuned and adapted to reproduce the network dynamics of the spontaneous activity displayed at different degrees of maturation and the stimulus evoked response.

The measured network is constituted by a small subset of neurons (up to 60 (Macis *et al* 2007)); each subset is coupled to a specific microelectrode, and such clustered neurons are interconnected among them.

The proposed model takes into account two important findings regarding the dynamics exhibited by patterned neuronal networks. First of all, enhancing the complexity of the meta-neurons morphology reflects the variations of the network dynamics as a function of the network development (cf figures 5(C) and (D)). Moreover, the obtained experimental results suggest a possible short- and long-term interaction among the clustered neurons that might be mediated by the subsets themselves. The model strengthens the hypothesis that direct connections (by means of neurite bundles) among not-neighbouring microelectrodes are also necessary, by showing that a simple OTN rule is not suitable to explain both the spontaneous (cf figure 6) and the evoked activity (cf figure 7(D)) of such a network. Thus, the obtained simulated results underline the presence of short- and long-term distance interactions to support the inherent dynamics of such interconnected neuronal populations.

The model was developed to be utilized when specific network topologies or patterned neuronal populations are used as experimental models. By using such models and the simulated results, it is possible to obtain useful indications for the design of specific network architectures. Theoretically, specific input–output functions or specific spontaneous dynamics can be estimated by simulating different network topologies and subsequently utilized to implement actual experimental models and hybrid systems with pre-defined features.

Acknowledgments

The authors are very grateful to Dr Valentina Pasquale for the thorough revision of the manuscript and her valuable suggestions. This work was supported by the Italian Ministry for the University and Research (MUR), PRIN2006.

References

Abeles M, Hayon G and Lehmann D 2004 Modeling compositionality by dynamic binding of synfire chains *J. Comput. Neurosci.* **17** 179–201

Carnevale N T and Hines M L 2005 *The NEURON Book* (Cambridge: Cambridge University Press)
Chang J C, Brewer G J and Wheeler B C 2001a Modulation of neural network activity by patterning *Biosens. Bioelectron.* **16** 527–33
Chang J C, Wheeler B C and Brewer G J 2001b Microelectrode array recordings of patterned hippocampal neurons for four weeks *Biomed. Microdevices* **2** 245–53
Chiappalone M, Bove M, Vato A, Tedesco M and Martinoia S 2006 Dissociated cortical networks show spontaneously correlated activity patterns during *in vitro* development *Brain Res.* **1093** 41–53
Claverol-Tinturé E, Ghirardi M, Fiumara F, Rossel X and Cabestany J 2005 Multielectrode arrays with elastometric microstructured overlays for extracellular recordings from patterned neurons *J. Neural. Eng.* **2** L1–7
Claverol-Tinturé E, Rossel X and Cabestany J 2007 Technical steps towards one-to-one electrode-neuron interfacing with neural circuits reconstructed in vitro *Neurocomputing* **70** 2716–22
Colquhoun D, Jonas P and Sakmann B 1992 Action of brief pulses of glutamate on AMPA/kainate receptors in patches from different neurones of rat hippocampal slices *J. Physiol.* **458** 261–87
Destexhe A, Mainen Z and Sejnowski T J 1994 An efficient method for computing synaptic conductances based on a kinetic model of receptor binding *Neural Comput.* **6** 14–8
Faisal A A, Selen L P J and Wolpert D M 2008 Noise in the nervous system *Nat. Rev. Neurosci.* **9** 292–303
Gerstner W 2003 *Integrate-and-Fire Neurons and Networks* 2nd ed (Cambridge, MA: MIT Press) pp 577–81
Giugliano M, Bove M and Grattarola M 1999 Activity-driven computational strategies of a dynamically regulated integrate-and-fire model neuron *J. Comput. Neurosci.* **7** 247–54
Hines M L and Carnevale N T 1997 The NEURON simulation environment *Neural Comput.* **9** 1179–209
Hodgkin A L and Huxley A F 1952 A quantitative description of membrane current and its applications to conduction and excitation in nerve *J. Physiol.* **117** 500–44
Izhikevich E M 2003 Simple model of spiking neurons *IEEE Trans. Neur. Net.* **6** 1569–72
Izhikevich E M, Gally J A and Edelman G M 2004 Spike-timing dynamics of neuronal groups *Cereb. Cortex* **14** 933–44
Jun S B, Hynd M R, Dowell-Mesfin N, Smith K L, Turner J N, Shain W and Kim S J 2007 Low-density neuronal networks cultured using patterned poly-l-lysine on microelectrode arrays *J. Neurosci. Methods* **160** 317–26
Kowalsi J M, Albert G L, Rhoades B M and Gross G W 1992 Neuronal networks with spontaneous, correlated bursting activity: theory and simulations *Neural Netw.* **5** 805–22
Latham P E, Richmond B J, Nirenberg S and Nelson P G 2000 Intrinsic dynamics in neuronal networks: I. Theory *J. Neurophysiol.* **83** 808–27
Liu B, Ma J, Gao E, He Y, Cui F and Xu Q 2008 Development of an artificial neuronal network with post-mitotic rat fetal hippocampal cells by polyethylenimine *Biosens. Bioelectron.* **23** 1221–8
London M, Meunier C and Segev I 1999 Signal transfer in passive dendrites with nonuniform membrane conductance *J. Neurosci.* **19** 8219–33
Macis E, Tedesco M, Massobrio P, Raiteri R and Martinoia S 2007 An automated microdrop delivery system for neuronal network patterning on microelectrode arrays *J. Neurosci. Methods* **161** 88–95
Marom S and Shahaf G 2002 Development, learning and memory in large random networks of cortical neurons: lessons beyond anatomy *Q. Rev. Biophys.* **35** 63–87
Massobrio P, Baljon P L, Maccione A, Chiappalone M and Martinoia S 2007 Activity modulation elicited by electrical stimulation in networks of dissociated cortical neurons *Conf. IEEE EMBS (IEEE, Lyon)* pp 3008–11
Mehring C, Hehl U, Kubo M, Diesmann M and Aertsen A 2003 Activity dynamics and propagation of synchronous spiking in locally connected random networks *Biol. Cybern.* **88** 395–408
Parga N and Abbot L F 2007 Network model of spontaneous activity exhibiting synchronous transitions between up and down states *Front. Neurosci.* **1** 57–66
Persi E, Horn D, Volman V, Segev R and Ben-Jacob E 2004 Modeling of synchronized bursting events: the importance of inhomogeneity *Neural Comput.* **16** 2577–95
Raichman N and Ben-Jacob E 2008 Identifying repeating motifs in the activation of synchronized bursts in cultured neuronal networks *J. Neurosci. Methods* **170** 96–110
Raichman N, Volman V and Ben-Jacob E 2006 Collective plasticity and individual stability in cultured neuronal networks *Neurocomputing* **69** 1150–54
Rieke F, Warland D, de Ruyter van Steveninck R and Bialek W 1997 *Spikes: Exploring the Neural Code* (Cambridge, MA: MIT Press)
Segev R and Ben-Jacob E 2001 Spontaneous synchronized bursting in 2D neural networks *Physica* A **302** 64–69
Segev I, Fleshman J W, Miller J P and Bunow B 1989 *Compartmental Models of Complex Neurons* (Cambridge, MA: (Bradford Book) MIT Press) pp 63–96
Shao J, Tsao T-H and Butera R 2006 Bursting without slow kinetics: a role for small world? *Neural Comput.* **18** 2029–35
Shin C-W and Kim S 2006 Self-organized criticality and scale-free properties in emergent functional neural networks *Phys. Rev.* E **74** 045101-1–4
Steinmetz P M, Manwani A, Koch C, London M and Segev I 2000 Subthreshold voltage noise due to channel fluctuations in active neuronal membranes *J. Comput. Neurosci.* **9** 133–48
Teramae J-N and Fukai T 2007 Local cortical circuit model inferred from power-law distributed neuronalavalaches *J. Comput. Neurosci.* **22** 301–12
Van Ooyen A, Duijnhouver J, Remme Michiel W H and Van Pelt J 2002 The effect of dendritic topology on firing patterns in model neurons *Netw.: Comput. Neural Syst.* **13** 311–25
Van Pelt J, Vajda I, Wolters P S, Corner M A and Ramakers G J A 2005 Dynamics and plasticity in developing neural networks *in vitro Prog. Brain Res.* **147**
Van Pelt J, Wolters P S, Corner M A, Rutten W L C and Ramakers G J A 2004 Long-term characterization of firing dynamics of spontaneous bursts in cultured neural networks *IEEE Trans. Biomed. Eng.* **51** 2051–62
Vogels T P and Abbot L F 2005 Signal propagation and logic gating in networks of integrate-and-fire neurons *J. Neurosci.* **16** 10786–95
Vogels T P, Rajan K and Abbot L F 2005 Neural network dynamics *Ann. Rev. Neurosci.* **28** 357–76
Volman V, Baruchi I, Persi E and Ben-Jacob E 2004 Generative modelling of regulated dynamical behavior in cultured neuronal networks *Physica* A **335** 249–78
Wagenaar D A, Madhavan R, Pine J and Potter S M 2005 Controlling bursting in cortical cultures with closed-loop multi-electrode stimulation *J. Neurosci.* **25** 680–8
Wagenaar D A, Pine J and Potter S M 2006 An extremely rich repertoire of bursting patterns during the development of cortical cultures *BMC Neurosci.* **7**
White J A, Rubinstein J T and Kay A R 2000 Channel noise in neurons *Trends Neurosci.* **23** 131–37